Research Article | Vol. 27, No. 11 | 27 May 2019 | OPTICS EXPRESS 15638
Optics EXPRESS

Greater than 50 times compression of 1030 nm Yb:KGW laser pulses to single-cycle duration

CHIH-HSUAN LU,[1,2,5] WEI-HSIN WU,[1] SHIANG-HE KUO,[1] JHAN-YU GUO,[1] MING-CHANG CHEN,[1,3,4] SHANG-DA YANG,[1] AND A. H. KUNG[1,2,6]

[1]*Institute of Photonics Technologies, National Tsing Hua University, Hsinchu, Taiwan*
[2]*Institute of Atomic and Molecular Sciences, Academia Sinica, Taipei, Taiwan*
[3]*Department of Physics, National Tsing Hua University, Hsinchu, Taiwan*
[4]*Frontier Research Center on Fundamental and Applied Sciences of Matters, National Tsing Hua University, Hsinchu, Taiwan*
[5]*lzch2000@hotmail.com*
[6]*akung@ee.nthu.edu.tw*

Abstract: Generation of octave-spanning spectrum that spans from 570 nm to 1300 nm utilizing 1030 nm 170 fs pulses from a Yb:KGW laser and a two-stage multiple-plate arrangement is demonstrated. 3.21 fs sub-single-cycle pulses are obtained after dispersion compensation. The high compression ratio of more than 50 times is achieved for two scenarios with widely different parameters including high input peak power at 1 kHz repetition rate and modest peak power at a high repetition rate of 100 kHz. The output pulses have good spatial mode quality and exhibit long-term stability. The achieved compression ratio and flexibility are unprecedented in ultrafast pulse compression to single-cycle regime. The experiments demonstrate that the technique of multiple-plate pulse compression is versatile and applicable for a wide range of laser pulse parameters.

1. Introduction

Intense single-cycle femtosecond pulses are ideal for generating bright isolated attosecond pulses via high-order harmonic generation (HHG) for attosecond science. These pulses enable the investigation of ultrafast electron dynamics with unprecedented temporal and spatial resolution [1–5]. So far chirped-pulse-amplified mode-locked Ti:sapphire laser systems have been the workhorse in providing intense few-to-single cycle pulses for these experiments. Ti:sapphire lasers typically operate at a few kHz repetition rate and an average power of less than 10 W. Yet it has become clear that for many of these studies as well as many emerging applications the optimal condition is for operating at a few hundred kHz repetition rate or at higher pulse energies than what is available from the Ti:sapphire laser [6]. It has also been found that scaling up the pulse repetition rate along with the average power is exceptionally challenging for the Ti:sapphire laser [7].

For this reason Yb-based lasers are receiving a lot of attention as an alternative laser source [8–10]. These lasers have been shown to scale in pulse repetition rate and in pulse energy to meet the conditions desired in many applications. However, the intrinsic duration of the Yb laser pulses is at least a few hundred femtoseconds, restricted by the bandwidth of the lasing transition. It is a necessity to compress the Yb laser pulses to shorter durations for them to become a viable replacement of the Ti:sapphire laser in ultrafast applications. The ultimate goal is to reach a duration of 3-4 fs which is equivalent to approximately a single cycle for a 1030 nm pulse.

Compared to compression of Ti:sapphire laser pulses, the Yb laser pulses present a different set of challenges because of the much longer pulse duration. Having longer pulses means requiring a larger ratio of compression to reach a few cycles. Meanwhile the longer

#363308 https://doi.org/10.1364/OE.27.015638
Journal © 2019 Received 29 Mar 2019; revised 10 May 2019; accepted 13 May 2019; published 17 May 2019

Optics EXPRESS

pulse leads to a lower damage threshold in materials, generating more ionized electrons, and more readily forming plasmas and filaments in the interaction of the pulse with a medium. The resulting lower operating intensity raises a need for a longer interaction length to achieve the same degree of spectral broadening in pulse compression which in turn leads to more undesirable effects. Overall this means that it is a bigger challenge to compress Yb laser pulses to a few optical cycles. There have been several reports on the compression of Yb laser pulses. They include compression of pulses from a mode-locked oscillator using bulk crystals [11], nonlinear compression in a multi-pass cell [12–15], pulse compression in a gas-filled kagome hollow-core photonic crystal fiber [16], employing a single hollow-core fiber [17–19], or compression of high-energy pulses by cascading two sets of thin fused-silica plates [20] and two-stage hollow-core fiber compression [21]. Most of these schemes could achieve compression to several optical cycles or 15-20 fs pulse duration. The best compression reported to this date is reduction to 5.1 fs, about 2 cycles in duration. The authors report it required using a hollow-core fiber of several meters long and a multi-mJ pulse [22]. The generation of single-cycle pulses from Yb laser systems and at high repetition rates has remained elusive.

Here we report the pulse compression of high power 1030 nm pulses from the initial pulse duration of 170 fs down to the single-cycle regime (3.21 fs) based on multiple-plate compression (MPC), which was first applied to single-cycle compression of 30 fs Ti:Sapphire 800nm pulses [23,24]. Spatio-spectral characterization of 800 nm compressed pulses using SEA-F-SPIDER shows there is only minor asymmetry in the two orthogonal polarization directions. A previous CEP stability test indicates that substantial spectral broadening induced by strong nonlinear interaction in the plates does not compromise the CEP characteristics [6]. The realization of polarization control of isolated high harmonic generation pulses driven by two compressed MPC pulses shows the reliable focusing quality of our approach [25]. So the multiple plates approach can be extended to compressing Yb laser pulses with significantly longer initial pulse duration to the single-cycle regime. This is achieved by employing a cascaded compression scheme consisting of two stages of compression using thin solid plates. The first stage pre-compresses the 170 fs pulses to circa 40 fs with high efficiency. A second stage completes compression of the pulses to single-cycle pulse duration. An overall compression ratio of 53 is achieved. The use of thin plates for compression has many benefits compared to alternate approaches. It is robust, reliable, easy to align, and preserves and often improves the spatial mode quality of the input laser pulse.

2. Generation of single-cycle-pulse in the multiple plate continuum setup

Here we present MPC compression in two different scenarios. One is MPC driven by high energy pulses running at a low repetition rate (1 mJ, 1 kHz), while the other is driven by relatively low energy pulses operating at a high repetition rate (60 μJ, 100kHz). It's aimed to demonstrate that MPC can work in a wide range of pulse energy from tens of μJ to mJ by simply changing the focusing, and the thickness and the spacing of plates.

2.1 MPC driven by 1 mJ pulses at a 1 kHz repetition rate

Figure 1 shows the two-stage multiple-plate continuum generator (MPC) plus compressor setup. The input laser is a 1030 nm 170 fs linearly-polarized Yb:KGW laser system (Light Conversion, PHAROS, PH1-SP-1.5 mJ). This laser operates from 1 kHz to more than 100 kHz repetition rate with a maximum pulse energy of 1.07 mJ (6.3 GW peak power), available at low kHz rep rates, and a maximum average power of 5.36 W. We begin the experiments by operating the laser at 1 kHz that gives the highest peak power. The laser pulse was focused to a $1/e^2$ waist of 0.31 mm to yield an intensity of 4.08 TW/cm^2 (calculated at normal incidence) at the entrance to the first quartz plate in the first MPC stage (Fig. 1). This intensity was chosen to maximize the generated spectral width while avoiding optical damage and filament formation inside the quartz plate. To record the resulting spectrum, a small portion of the

Optics EXPRESS

output beam is delivered to a fiber-coupled optical spectrometer equipped with an InGaAs array detector (B&W Tek, Sol 1.7). The quartz plates used throughout this entire report are z-cut, 1x2 cm^2 rectangular plates and are placed at Brewster's angle to the incident beam.

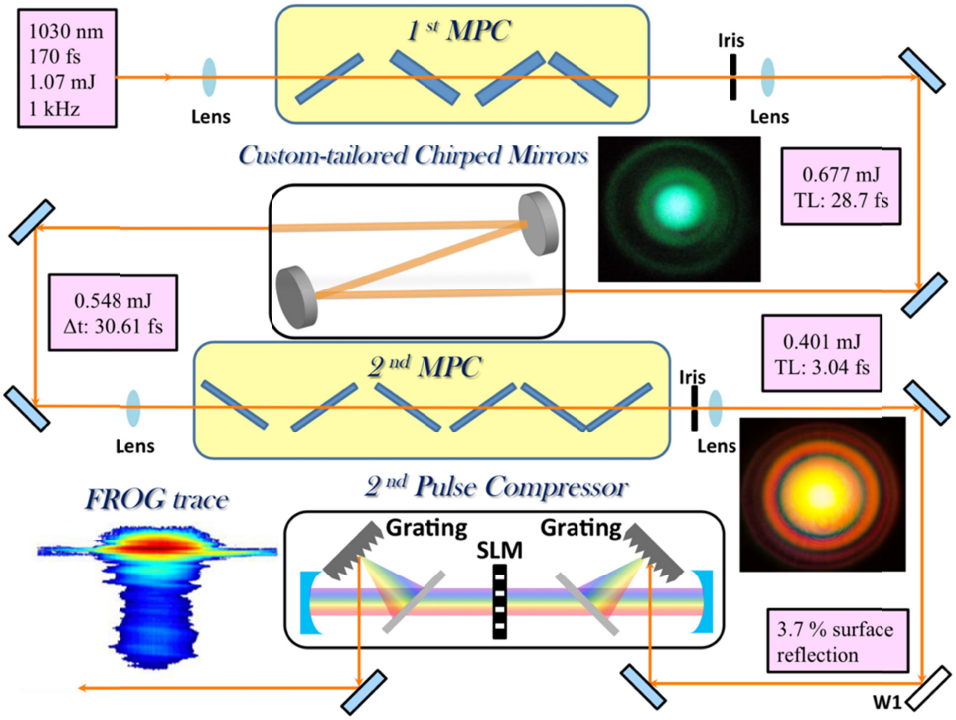

Fig. 1. Schematic of the experimental setup of two-stage pulse compression using multiple thin plates at 1 kHz repetition rate. The beam profiles of photographic images are recorded at 1 m after the collimated lens in the first (top) and second (bottom) MPC stages respectively. Note that the beam profile is taken when the iris is fully opened. SLM: spatial light modulator. TL: transform limited pulse duration. W1 is an uncoated wedge that reflects 3.7% of the incident light to prevent optical damage to the SLM (Jenoptik, SLM-S640).

The first plate in this first stage is 200 μm thick. At this thickness, the input induced nonlinear phase is estimated to be 0.44 π radians, in concurrence with the guideline provided by Cheng et. al. [26]. For the second plate we find that a 200 μm thicker plate tends to damage after a short time whereas a plate coupled with a corresponding lower intensity on the plates and an increased spacing between plates eliminates the damage problem but continues to broaden the spectrum. The procedure to place this and subsequent plates (all 400 μm thick) followed that outlined in our earlier report [23]. A total of four plates were used that result in a spectral width that meets the goal for this stage which is to reduce the pulse duration to 30-40 fs. The spacing between adjacent plates was measured to be 16 cm, 16 cm, and 13.5 cm, respectively. Figure 2(a). shows the pulse spectrum recorded after every plate insertion in the first MPC stage. The figure indicates that for these relatively long pulses the pulse spectrum broadens incrementally after passing through each plate. The broadening mechanism is dominated by spatiotemporal self-focusing and self-phase modulation. After the fourth plate, a −20 dB bandwidth from 960 nm to 1080 nm is obtained. The conical emission associated with the generation was filtered with an iris aperture and the remaining beam was collimated with a 1.5 m focal length spherical mirror. The energy of this central portion was 677 μJ per pulse (63.2% energy conversion). The pulse power was stable and durable (Fig. 2(b)). In this case we used less intensity to demonstrate this result as well as have shown the long-term stability (10 hours per day, 5 days a week and continue testing for more than 3 months with

Optics EXPRESS

the same plates), presenting that the plate would not be damaged under such intensity. It is possible to obtain a broader spectrum that supports transform-limited (TL) pulse duration down to 20 fs by using a couple more plates and shortening the spacing between plates. However doing so simultaneously leads to excessive conical emission (i.e. lower energy conversion) and flicker in the beam intensity. Therefore, we consider four plates being the optimal case for this stage.

The pulse coming out of the MPC is severely chirped. Hence the pulse from the first stage was bounced (twice) off a custom-tailored chirped mirror that has been coated using the phase information of the spectral-broadened pulse; information obtained using spectral phase interferometry. The pulses are then characterized using a homemade polarization-gating crossed frequency-resolved optical-gating (PG-XFROG) apparatus [27]. The pulse envelope curves reported throughout this paper are reconstructed from FROG traces of 480 × 1500 grid size and have a typical FROG error of 0.25%. FROG reconstruction shows that the compressed pulse from the first stage has an intensity FWHM of 30.6 fs (TL pulse width is 28.7 fs) shown in Fig. 3(b). The pulse energy was 638 μJ. The reconstructed temporal pulse envelope closely resembles the TL pulse but has a residual tail that likely is due to high-order dispersion not completely compensated by the chirped mirrors.

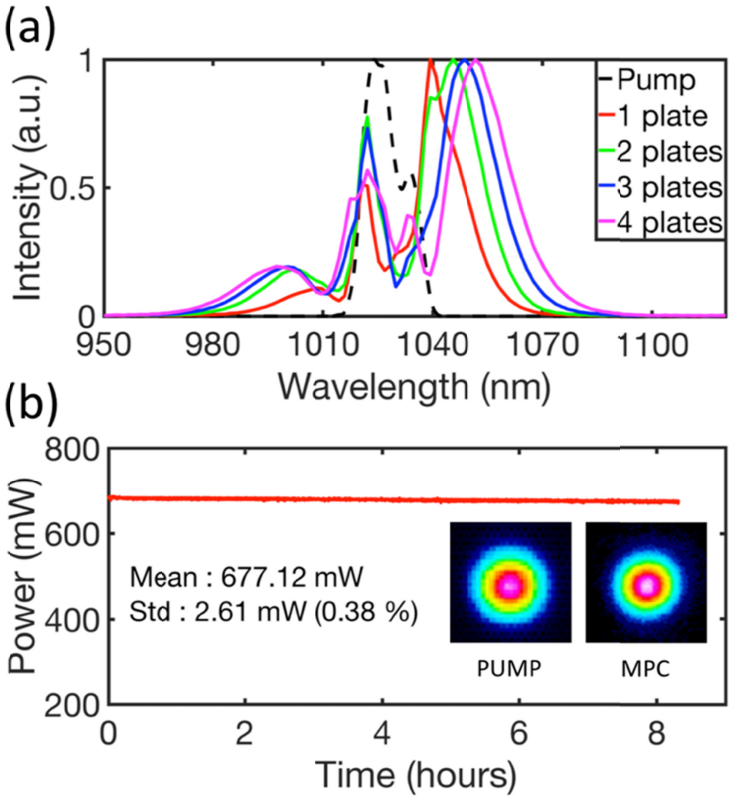

Fig. 2. (a) Spectral broadening as a result of different number of plates in the first MPC stage. (b) The output power of the first MPC stage measured over 8 hours. The left inset shows the focusing beam profile of the incident pulses, while the right inset represents the MPC focusing profile.

Optics EXPRESS

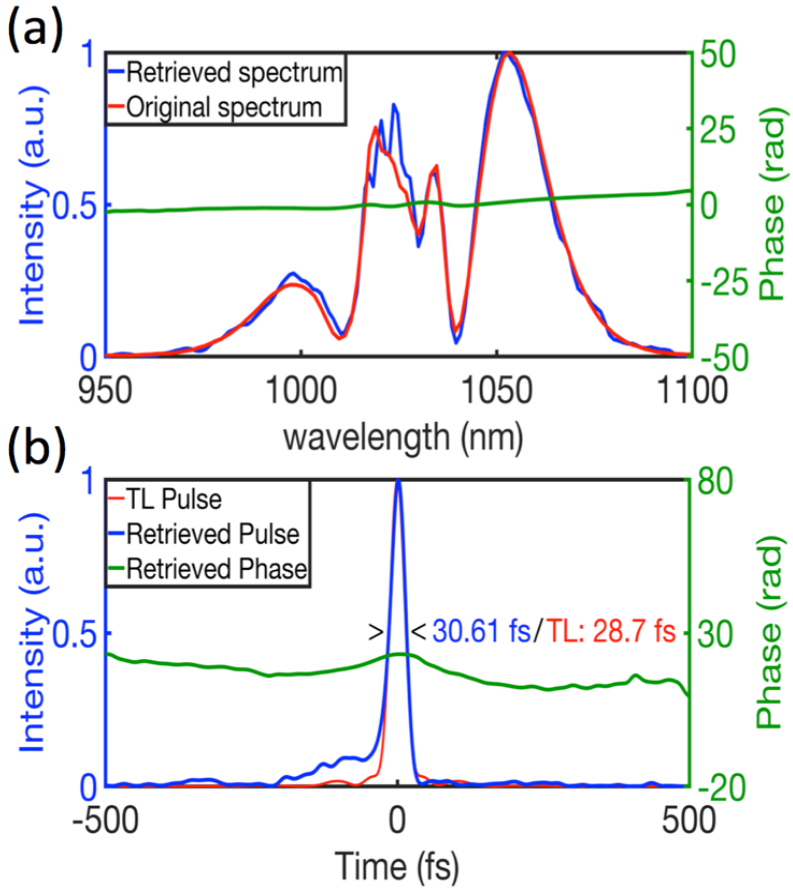

Fig. 3. PG-XFROG measurement of compressed MPC after two bounces off custom-tailored chirped mirrors. (a) Reconstructed spectral intensity (blue) and spectral phase (green), and the original spectrum recorded by a spectrometer (red). (b) Reconstructed temporal intensity (blue) and phase (green) of the pulse. It shows that the pulse is compressed close to the TL-pulse. The final FWHM of the intensity profile is 30.6 fs.

The pulse energy drops from 638 μJ to 548 μJ due to reflection loss at 4 silver surfaces at the beam directing and focusing optics used to send the pulse into the second MPC stage. In the second MPC stage, we used an intensity of 10.4 TW/cm^2 (normal incidence value) and 100 μm thick quartz plates. The calculated peak nonlinear phase shift was 0.49 π. Six plates were employed for maximum broadening. The optimized spacing between the plates was 7.8 cm, 6 cm, 5 cm, 3.7 cm, and 2.8 cm respectively. The spetrum after the sixth plate covers from 570 nm to 1300 nm at –20 dB intensity level. Since the spectrum straddles the visible to the near-IR, two spectrometers equipped with a Si and an InGaAs array detectors were used to record the full spectrum. Figure 4(a) shows the spectra recorded for the different number of plates used respectively. Every spectrum is obtained by stitching the measurements from the two spectrometers together. The spectra expand gradually but quite symmetrically in the first three plates, signaling that broadening is mainly from self-phase modulation. The spectra expand rapidly to the blue in the next three plates. This is evidence that self-steepening has become significant in this stage, caused by the shorter incident pulse. The final spectrum supports a TL duration of 3.08 fs. After the second MPC stage the spatial mode of the beam remains about the same as after the first MPC stage, as can be seen in the photographic images of the beam profile shown in Fig. 1 and CCD far-field images in Fig. 2 and Fig. 4.

The output pulse energy after removing the outer ring by an iris of the second MPC stage was 401 μJ and represents a 73% conversion for this stage. Excellent longevity of the MPC is demonstrated by uninterrupted operation of over 8 hours (Fig. 4(b)). In the first MPC stage, we used a 2.25 m focusing lens to focus the pump to the first plate, and a 1.5 m focusing lens was used to collimate the MPC output. In the second MPC stage, we used a 2 m lens to focus the collimated 1st MPC output to 2nd MPC stage, the octave spanning output is collimated by using a 1.5 m concave mirror. In the 1 kHz setup (pulse energy of ~mJ), the overall optical path of the 1st MPC plus the 2nd MPC is roughly 8 m long.

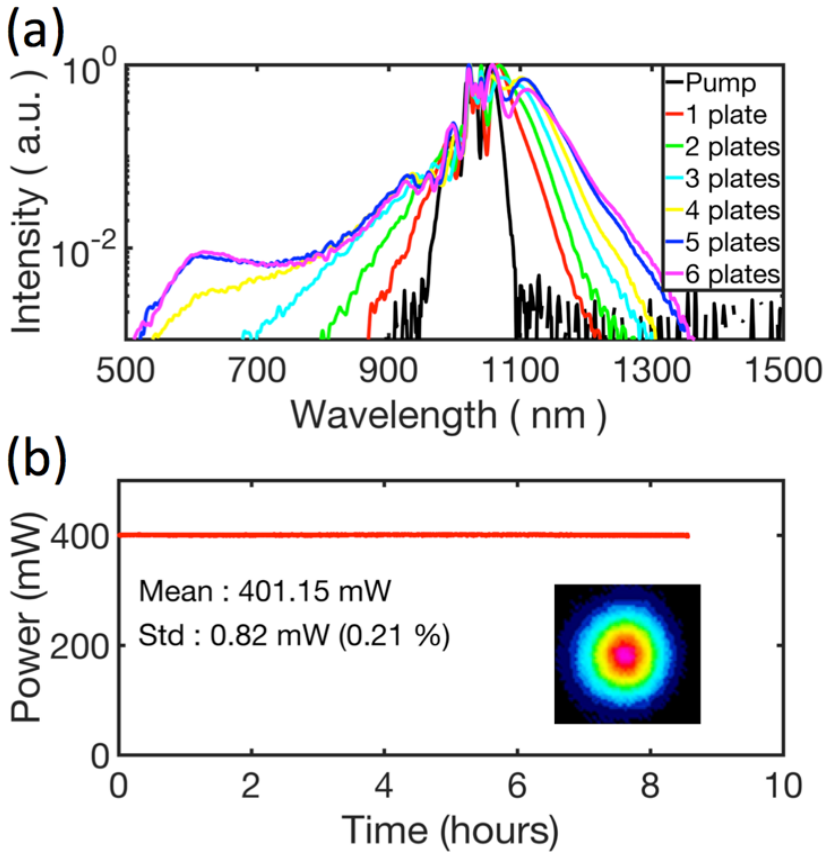

Fig. 4. (a) Spectral broadening in log scale with different number of plates in the second MPC stage. (b) Power measurement showing good long-term stability over more than 8 hours.

2.2 MPC driven by 60 μJ,pulses at a 100 kHz repetition rate

The next experiment is to test cascaded MPC at 100 kHz pulse repetition rate. At this repetition rate the pulse peak power is 0.31 GW (53.6 μJ in 170 fs), 20 times weaker than that at 1 kHz. We focused this power to an intensity of 1.84 TW/cm^2, a factor of 2.2 smaller than that at 1 kHz MPC generation, but is more practical because the Rayleigh range is such that it leaves more room to place the subsequent plates (focused waist 0.1 mm, Rayleigh range 3.1 cm). To compensate for this lowered intensity we increased the quartz plate thickness to 800 μm. After 5 plates with spacings of 2.1 cm, 1.8 cm, 1.5 cm, and 1.5 cm respectively the pulse spectrum is broadened to the magenta curve shown in Fig. 5(a). Once again self-phase modulation is the dominant broadening mechanism in this first stage.

Optics EXPRESS

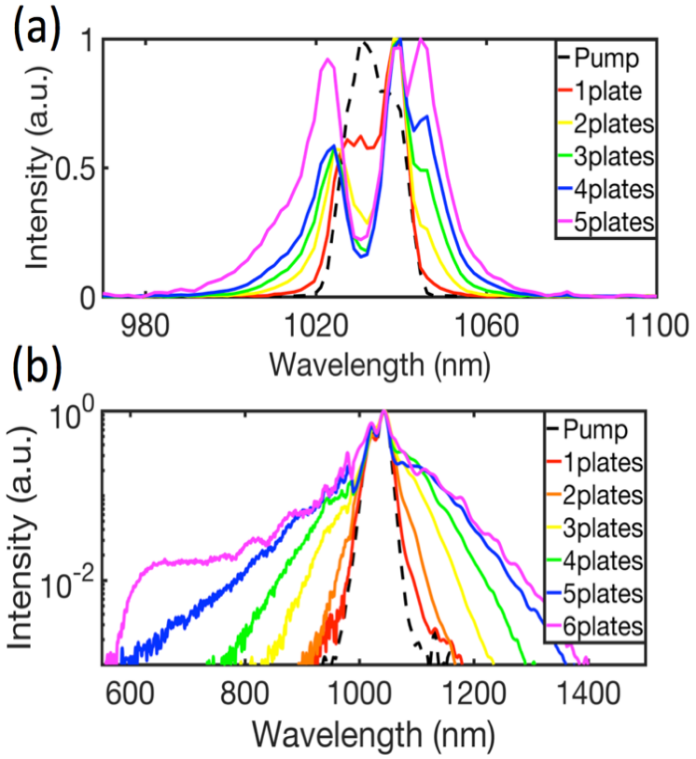

Fig. 5. Spectral broadening with different number of plates in the (a) first, and (b) second MPC stage, respectively. Spectra in (a) was recorded in an InGaAs spectrometer, and in (b) in both InGaAs and Si spectrometers.

A pair of chirped mirrors similar to the one used in the 1 kHz case compressed the pulse to 40 fs (characterized by PG-XFROG). Significantly in this case the pulse has a negligible high-order tail in the temporal profile (Fig. 6(b)). We attribute this to the lower input intensity that leads to a weaker high-order nonlinearity. The pulse energy was 47 μJ representing a 87.5% conversion from the input pulse energy. This conversion is the highest we have seen in our experience working on MPC. Unfortunately, the pulse energy dropped to 34.2 μJ after several reflections off silver mirrors needed in the present setup for the second 100 kHz MPC stage. We note here that most of the energy losses reported here from reflecting optics could be recovered with improved mirror reflectivity in future experiments. For this second stage the intensity incident onto the first quartz plate was 4.6 TW/cm^2. In accordance with this intensity, plates 200 μm thick were used for the experiment. The pulse spectrum reached a maximum width (at −20 dB) after six plates. The spacing between adjacent plates for the six plates was 6 mm, 5 mm, 4 mm, 3 mm, and 2.5 mm respectively. At this point the energy of the pulse after filtering out the conical emission was 21.6 μJ. This is a 63.1% energy conversion for this MPC stage. The average power of the output came to 2.16 W. Once again the spatial mode of the output beam remains near Gaussian. There is no evidence of thermal distortion. With broadband dielectric mirrors and improved mirror reflectivity we expect the octave-spanning pulse energy to reach 27 μJ that would yield a net 50% energy conversion from the 170 fs pulse. The final spectrum spans from 600 nm to 1300 nm at −20 dB level (Fig. 5(b)). This spectrum supports a TL pulse width of 3.77 fs. Such a pulse should be useful for high-resolution temporal measurements as well as isolated attosecond pulse generation via high-order harmonics generation, and many other applications at 100 kHz repetition rate.

Optics EXPRESS

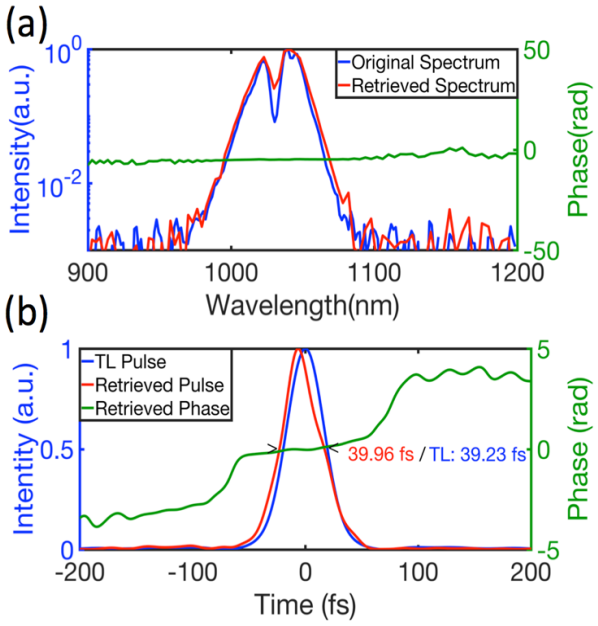

Fig. 6. PG-XFROG measurement of 100 kHz compressed pulses after the first MPC stage. (a) Reconstructed spectral intensity (red) and spectral phase (green); spectrum as it is recorded by an InGaAs spectrometer (blue). (b) Reconstructed temporal intensity (red) and phase (green) of the pulse.

2.3 Compression of pulses after the second MPC stage

Phase compensation of pulses that have an octave-spanning spectrum requires special attention due to the large high-order nonlinearity that is associated with acquiring the broad spectrum. Commercial chirped mirrors primarily designed to compensate second order spectral phase in fused silica are not sufficient to do the job. Custom-designed chirped mirrors are required and they are not yet available. Nevertheless, in order to demonstrate compression of these broadband pulses we took a 3.7% portion of the octave-spanning pulse from the 1 kHz experiment and sent it through a 4-f spatial-light-modulator (SLM) pulse shaper to actively compensate the spectral phase (see Fig. 1). The large reduction in pulse energy used is in consideration of potential damage to the liquid crystal layer in the SLM. Figure 7 shows the pulse reconstructed from PG-XFROG after phase compensation. The FWHM of the temporal intensity envelope has been compressed to 3.21 fs. The corresponding electric field is less than one optical cycle (at a carrier wavelength of 1030 nm the single-cycle intensity envelope width is 3.43 fs). There is concern on the accuracy of this measurement that originates from the width of the gate pulse used and the intrinsic limitation of the FROG technique when the pulse approaches the single-cycle limit. We cross-checked our results using gate pulse of width 170 fs from the laser as well as with 30.6 fs pulses from the first stage after compression. The resulting pulse widths from the two measurements agree to within 2%. For better certainty of the pulse width it will be useful to employ the optical streaking technique to confirm the actual field profile [28]. This is being developed and will be reported in the near future. The energy of the compressed pulse obtained thusly was 5 μJ, limited mainly by the diffraction efficiency of the two gratings (53004FS06-396R) used in the phase compensator. We expect that more than 90% of the broadened pulse energy can be recovered after compression when appropriate broadband chirped mirrors become available for phase compensation so that when optimized single-cycle pulses of more than 400 μJ (125 GW peak power) at 1 kHz and 25 μJ per pulse (7.8 GW peak power) at 100 kHz rep rate could be available.

Optics EXPRESS

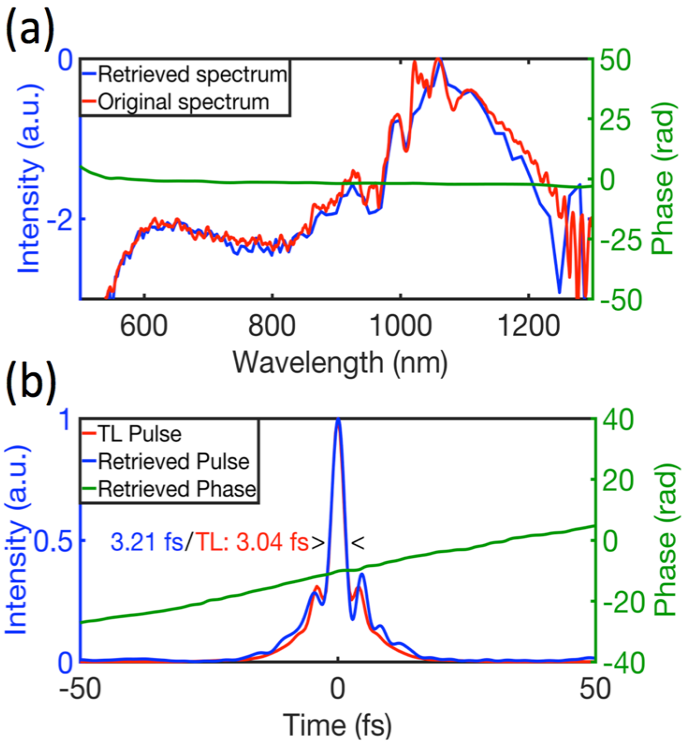

Fig. 7. PG-XFROG measurement of compressed pulse after the second 1 kHz MPC stage. (a) Reconstructed spectral intensity (blue) and spectral phase (green). The original spectrum was recorded by a spectrometer (red) (b) Reconstructed temporal intensity (blue) and phase (green) of the pulse. The FWHM of the reconstructed intensity envelope is 3.21 fs.

3. Conclusion

In summary we have demonstrated generation of single-cycle pulses and achieved greater than 50 times pulse compression of 1030 nm 170 fs laser pulses using a two-stage multiple-plate technique. We also demonstrated the flexibility in repetition rate, pulse energy and pulse duration that the MPC technique permits in femtosecond pulse compression. The achieved compression ratio and flexibility are unprecedented in ultrafast pulse compression to single-cycle pulse regime. These experiments show that multiple-plate continuum generation is a uniquely capable and reliable technique for developing new light sources of the next generation. Extension of this technique to concurrent high repetition rate and high power operation can be anticipated. Such intense, stable, few to single-cycle laser pulses should enable many high impact applications and investigations in ultrafast dynamics, material processing, high field physics, and extreme nonlinear optics.

Funding

The Ministry of Science and Technology of Taiwan (MOST 105-2112-M-007-030, 107-2112-M-007-006, 108-2636-M-007 –001) and the Academia Sinica of Taiwan.

Acknowledgments

We thank Pei-Chi Huang for discussion, Chia-Lun Tsai and Yi-Hsun Tseng for assistance with the laser system.

Optics EXPRESS

References

1. S. R. Leone, C. W. McCurdy, J. Burgdorfer, L. S. Cederbaum, Z. Chang, N. Dudovich, J. Feist, C. H. Greene, M. Ivanov, R. Kienberger, U. Keller, M. F. Kling, Z. H. Loh, T. Pfeifer, A. N. Pfeiffer, R. Santra, K. Schafer, A. Stolow, U. Thumm, and M. J. J. Vrakking, "What will it take to observe processes in 'real time'?" Nat. Photonics **8**(3), 162–166 (2014).
2. D. Fabris, T. Witting, W. A. Okell, D. J. Walke, P. Matia-Hernando, J. Henkel, T. R. Barillot, M. Lein, J. P. Marangos, and J. W. G. Tisch, "Synchronized pulses generated at 20 eV and 90 eV for attosecond pump–probe experiments," Nat. Photonics **9**(6), 383–387 (2015).
3. D. D. Hickstein, F. J. Dollar, P. Grychtol, J. L. Ellis, R. Knut, C. Hernández-García, D. Zusin, C. Gentry, J. M. Shaw, T. Fan, K. M. Dorney, A. Becker, A. Jaroń-Becker, H. C. Kapteyn, M. M. Murnane, and C. G. Durfee, "Non-collinear generation of angularly isolated circularly polarized high harmonics," Nat. Photonics **9**(11), 743–750 (2015).
4. F. Lépine, M. Ivanov, and M. J. J. Vrakking, "Attosecond molecular dynamics: fact or fiction?" Nat. Photonics **8**(3), 195–204 (2014).
5. F. Krausz and M. I. Stockman, "Attosecond metrology: from electron capture to future signal processing," Nat. Photonics **8**(3), 205–213 (2014).
6. C. H. Lu, T. Witting, A. Husakou, M. J. J. Vrakking, A. H. Kung, and F. J. Furch, "Sub-4 fs laser pulses at high average power and high repetition rate from an all-solid-state setup," Opt. Express **26**(7), 8941–8956 (2018).
7. F. J. Furch, T. Witting, A. Giree, C. Luan, F. Schell, G. Arisholm, C. P. Schulz, and M. J. J. Vrakking, "CEP-stable few-cycle pulses with more than 190 μJ of energy at 100 kHz from a noncollinear optical parametric amplifier," Opt. Lett. **42**(13), 2495–2498 (2017).
8. A. Giesen, H. Hugel, A. Voss, K. Wittig, U. Brauch, and H. Opower, "Scalable concept for diode-pumped high-power solid-state lasers," Appl. Phys. B **58**(5), 365 (1994).
9. J. Aus der Au, G. J. Spühler, T. Südmeyer, R. Paschotta, R. Hövel, M. Moser, S. Erhard, M. Karszewski, A. Giesen, and U. Keller, "16.2-W average power from a diode-pumped femtosecond Yb:YAG thin disk laser," Opt. Lett. **25**(11), 859–861 (2000).
10. F. Röser, J. Rothhard, B. Ortac, A. Liem, O. Schmidt, T. Schreiber, J. Limpert, and A. Tünnermann, "131 W 220 fs fiber laser system," Opt. Lett. **30**(20), 2754–2756 (2005).
11. M. Seidel, G. Arisholm, J. Brons, V. Pervak, and O. Pronin, "All solid-state spectral broadening: an average and peak power scalable method for compression of ultrashort pulses," Opt. Express **24**(9), 9412–9428 (2016).
12. J. Schulte, T. Sartorius, J. Weitenberg, A. Vernaleken, and P. Russbueldt, "Nonlinear pulse compression in a multi-pass cell," Opt. Lett. **41**(19), 4511–4514 (2016).
13. J. Weitenberg, A. Vernaleken, J. Schulte, A. Ozawa, T. Sartorius, V. Pervak, H.-D. Hoffmann, T. Udem, P. Russbüldt, and T. W. Hänsch, "Multi-pass-cell-based nonlinear pulse compression to 115 fs at 7.5 μJ pulse energy and 300 W average power," Opt. Express **25**(17), 20502–20510 (2017).
14. L. Lavenu, M. Natile, F. Guichard, Y. Zaouter, X. Delen, M. Hanna, E. Mottay, and P. Georges, "Nonlinear pulse compression based on a gas-filled multipass cell," Opt. Lett. **43**(10), 2252–2255 (2018).
15. M. Ueffing, S. Reiger, M. Kaumanns, V. Pervak, M. Trubetskov, T. Nubbemeyer, and F. Krausz, "Nonlinear pulse compression in a gas-filled multipass cell," Opt. Lett. **43**(9), 2070–2073 (2018).
16. F. Emaury, C. J. Saraceno, B. Debord, D. Ghosh, A. Diebold, F. Gèrôme, T. Südmeyer, F. Benabid, and U. Keller, "Efficient spectral broadening in the 100-W average power regime using gas-filled kagome HC-PCF and pulse compression," Opt. Lett. **39**(24), 6843–6846 (2014).
17. B. H. Chen, M. Kretschmar, D. Ehberger, A. Blumenstein, P. Simon, P. Baum, and T. Nagy, "Compression of picosecond pulses from a thin-disk laser to 30fs at 4W average power," Opt. Express **26**(4), 3861–3869 (2018).
18. L. Lavenu, M. Natile, F. Guichard, Y. Zaouter, M. Hanna, E. Mottay, and P. Georges, "High-energy few-cycle Yb-doped fiber amplifier source based on a single nonlinear compression stage," Opt. Express **25**(7), 7530–7537 (2017).
19. X. Guo, S. Tokita, K. Yoshii, H. Nishioka, and J. Kawanaka, "Generation of 300 nm bandwidth 0.5 mJ pulses near 1 μm in a single stage gas filled hollow core fiber," Opt. Express **25**(18), 21171–21179 (2017).
20. J. E. Beetar, S. Gholam-Mirzaei, and M. Chini, "Spectral broadening and pulse compression of a 400 μJ, 20 W Yb:KGW laser using a multi-plate medium," Appl. Phys. Lett. **112**(5), 051102 (2018).
21. S. Hädrich, M. Kienel, M. Müller, A. Klenke, J. Rothhardt, R. Klas, T. Gottschall, T. Eidam, A. Drozdy, P. Jójárt, Z. Várallyay, E. Cormier, K. Osvay, A. Tünnermann, and J. Limpert, "Energetic sub-2-cycle laser with 216 W average power," Opt. Lett. **41**(18), 4332–4335 (2016).
22. Y.-G. Jeong, R. Piccoli, D. Ferachou, V. Cardin, M. Chini, S. Hädrich, J. Limpert, R. Morandotti, F. Légaré, B. E. Schmidt, and L. Razzari, "Direct compression of 170-fs 50-cycle pulses down to 1.5 cycles with 70% transmission," Sci. Rep. **8**(1), 11794 (2018).
23. C. H. Lu, Y. J. Tsou, H. Y. Chen, B. H. Chen, Y. C. Cheng, S. D. Yang, M. C. Chen, C. C. Hsu, and A. H. Kung, "Generation of intense supercontinuum in condensed media," Optica **1**(6), 400–406 (2014).
24. C. H. Lu, B. H. Chen, Y. C. Cheng, and A. H. Kung, in High-Brightness Sources and Light-Driven Interactions, "Multi-plate generation and compression of an intense supercontinuum pulse,"OSA Technical Digest (online) (Optical Society of America, 2016), paper HS4B.1.

Optics EXPRESS

25. P. C. Huang, C. H. García, J. T. Huang, P. Y. Huang, C. H. Lu, L. Rego, D. D. Hickstein, J. L. Ellis, A. J. Becker, A. Becker, S. D. Yang, C. G. Durfee, L. Plaja, H. C. Kapteyn, M. M. Murnane, A. H. Kung, and M. C. Chen, "Polarization control of isolated high-harmonic pulses," Nat. Photonics **12**(6), 349–354 (2018).
26. Y. C. Cheng, C. H. Lu, Y. Y. Lin, and A. H. Kung, "Supercontinuum generation in a multi-plate medium," Opt. Express **24**(7), 7224–7231 (2016).
27. T. C. Wong, M. Rhodes, and R. Trebino, "Single-shot measurement of the complete temporal intensity and phase of supercontinuum," Optica **1**(2), 119–124 (2014).
28. E. Goulielmakis, M. Uiberacker, R. Kienberger, A. Baltuska, V. Yakovlev, A. Scrinzi, T. Westerwalbesloh, U. Kleineberg, U. Heinzmann, M. Drescher, and F. Krausz, "Direct measurement of light waves," Science **305**(5688), 1267–1269 (2004).